Trivalent Ion Conduction in Molybdates Having $Sc_2(WO_4)_3$-Type Structure

Nobuhito Imanaka, Tomohiro Ueda, Yusuke Okazaki, Shinji Tamura, and Gin-ya Adachi*

Department of Applied Chemistry, Faculty of Engineering, Osaka University, 2-1 Yamadaoka, Suita, Osaka 565-0871, Japan

Received September 16, 1999. Revised Manuscript Received April 13, 2000

A molybdate series with $Sc_2(WO_4)_3$-type structure, which has been demonstrated to be suitable for trivalent ion conduction, was prepared, and the trivalent ion conducting characteristics of this series were compared with those of the tungstate series. The ionic conductivities of the molybdate series become considerably higher in comparison to those of the tungstate series. Since the ionic radius of Mo^{6+} is smaller than that of W^{6+}, the oxide anions that form a tetrahedron unit with Mo^{6+} ion form stronger bonds than those that form a tetrahedron unit with W^{6+}. Stronger hexavalent cation and oxide anion bonding develops more suitable surroundings for trivalent ion migration in the $Sc_2(WO_4)_3$-type structure. The trivalent ion conducting properties in the molybdate solids were directly characterized by dc electrolysis and EPMA measurements.

Introduction

Tungstates with trivalent ions such as aluminum,[1−5] indium,[6] and rare earths[7−13] have been demonstrated to be trivalent ion conductors. The tungstate solid electrolytes have $Sc_2(WO_4)_3$-type structure, which is a quasi-two-dimensional layered structure[14−17] that is suitable for ions of such high-valence cation species as trivalent ions. Various polycrystalline tungstate single phases and also single crystals, in addition to the tungstate solid solution phases with $Sc_2(WO_4)_3$-type structure, were comprehensively investigated and the trivalent ion conducting behaviors in $Sc_2(WO_4)_3$-type structure were clarified.[1−13]

In the tungstate structure, the hexavalent tungsten ion (W^{6+}) functions as a key element in realizing trivalent ion conduction. The W^{6+} cation forms a WO_4^{2-} unit and the cation bonds to four oxide ions in the tetrahedron. The strong bonding between W^{6+} and O^{2-} results in a release of the remaining trivalent ions under conditions that allow migration to proceed much more smoothly. From our previously reported research,[1−13] the existence of the higher valency cations as one of the components having a higher valency than the mobile ion is essential to obtain multivalent ion conductors. However, the disadvantage of the tungstate trivalent ion conductors is their relatively low ionic conductivity. One suitable way of enhancing the trivalent ion conductivity is to substitute the hexavalent W^{6+} cation for another hexavalent cation species.

Molybdenum also has a hexavalent state and the ionic radius of Mo^{6+} (0.055 nm[18]) is smaller than that of W^{6+} (0.056 nm[18]). Reduction of ionic radius, while maintaining the same hexavalent state results in a stronger bonding to the anions comprising the tetrahedron (MO_4^{2-}) units in $Sc_2(WO_4)_3$-type structure. As a result, the mobility of the trivalent ions in the molybdates with $Sc_2(WO_4)_3$-type structure are enhanced compared to those in the tungstate series.

In the present study, various types of molybdates, $M_2(MoO_4)_3$ (M = Al, In, Sc, Er, Tm, Yb, and Lu), which form with the same crystal structure as $Sc_2(WO_4)_3$, were selected as another suitable candidate series, and the trivalent ion conduction behaviors were investigated extensively for the series of the molybdates. The results obtained for the molybdates were compared in detail

* To whom all correspondence should be addressd.

(1) Kobayashi, Y.; Egawa, T.; Tamura, S.; Imanaka, N.; Adachi, G. *Chem. Mater.* **1997**, *9*, 1649.
(2) Tamura, S.; Egawa, T.; Okazaki, Y.; Kobayashi, Y.; Imanaka, N.; Adachi, G. *Chem. Mater.* **1998**, *10*, 1958.
(3) Imanaka, N.; Hiraiwa, M.; Tamura, S.; Adachi, G.; Dabkowska, H.; Dabkowski, A.; Greedan, J. E. *Chem. Mater.* **1998**, *10*, 2542.
(4) Köhler, J.; Kobayashi, Y.; Imanaka, N.; Adachi, G. *Solid State Ionics* **1998**, *113−115*, 553.
(5) Imanaka, N.; Kobayashi, Y.; Tamura, S.; Adachi, G. *Electrochem. Solid-State Lett.* **1998**, *1*, 271.
(6) Köhler, J.; Imanaka, N.; Adachi, G. *Z. Anorg. Allg. Chem.* **1999**, *625*, 1890.
(7) Imanaka, N.; Kobayashi, Y.; Adachi, G. *Chem. Lett.* **1995**, 433.
(8) Imanaka, N.; Adachi, G. *J. Alloys Compd.* **1997**, *250*, 492.
(9) Imanaka, N.; Kobayashi, Y.; Fujiwara, K.; Asano, T.; Okazaki, Y.; Adachi, G. *Chem. Mater.* **1998**, *10*, 2006.
(10) Kobayashi, Y.; Egawa, T.; Okazaki, Y.; Tamura, S.; Imanaka, N.; Adachi, G. *Solid State Ionics* **1998**, *111*, 59.
(11) Köhler, J.; Imanaka, N.; Adachi, G. *Chem. Mater.* **1998**, *10*, 3790.
(12) Tamura, S.; Imanaka, N.; Adachi, G. *Adv. Mater.* **1999**, *11*, 64.
(13) Kobayashi, Y.; Egawa, T.; Tamura, S.; Imanaka, N.; Adachi, G. *Solid State Ionics* **1999**, *118*, 325.
(14) Abrahams, S. C.; Bernstein, J. L. *J. Chem. Phys.* **1966**, *45*, 2745.
(15) Nassau, K.; Levinstein, H. J.; Loiacono, G. M. *J. Phys. Chem. Solids* **1965**, *26*, 1805.
(16) Borchardt, H. J. *J. Chem. Phys.* **1963**, *39*, 504.
(17) Nassau, K.; Shiever, J. W.; Keve, E. T. *J. Solid State Chem.* **1971**, *3*, 411.
(18) Shannon, R. D. *Acta Crystallogr.* **1976**, *A32*, 751.

10.1021/cm990591w CCC: $19.00
Published on Web 06/20/2000

with those reported for the tungstates having $Sc_2(WO_4)_3$-type structure.[9]

Experimental Section

Sample Preparation. Rare earth molybdates, $R_2(MoO_4)_3$ (R = Sc, Er, Tm, Yb, and Lu), were prepared by a conventional solid-state reaction. Stoichiometric amounts of R_2O_3 (purity: 99.9%) and MoO_3 (purity: 99.9%) were mixed in a mortar and calcined on a mullite boat at 700−1000 °C for 5−17 h in air. The calcined powder was ground and reheated at 1000−1100 °C for 12 h in air. The resulting powder was made into pellets (10 mm in diameter, 0.6−0.8 mm in thickness) and sintered at 1000−1100 °C for 12 h in air. In the case that the compounds of heavy rare earths, Er−Lu, the sample powder was dried in a vacuum at 150 °C before sintering because of the considerably high hygroscopic nature of these compounds. $Al_2(MoO_4)_3$ pellets were synthesized by heating a stoichiometric mixture of $Al(OH)_3$ (purity: 99.99%) and MoO_3 at 700 °C for 5 h, 800 °C for 12 h and then sintered at 800 °C for 12 h in air. $In_2(MoO_4)_3$ was prepared by mixing In_2O_3 (purity: 99.9%) and MoO_3 in a stoichiometric ratio and then heating at 700 °C for 5 h and 800 °C for 12 h. The sintering of the $In_2(MoO_4)_3$ pellets was done at 800 °C for 12 h. The $Al_2(MoO_4)_3$−$Sc_2(MoO_4)_3$ solid solutions were prepared by mixing each molybdate in a stoichiometric ratio and then heating at 700 °C for 5 h and 800 °C for 12 h, and then sintering at 800 °C for 12 h.

The samples were identified by X-ray powder diffractometer using Cu Kα radiation (M18XHF, Mac Science). The XRD data were collected by a step-scanning method in the 2θ range from 10° to 70° using a step width of 0.04° and a scan time of 4 s. The XRD data were analyzed using the Rietveld refinement program RIETAN-94.[19]

Conducting Property Measurements. Electrical conductivity was measured by both an ac method and dc method, using the sintered ceramic pellet and two platinum electrodes in the temperature range from 200 to 600 °C. The ac conductivity measurements were performed via an ac complex impedance method in the frequency range from 20 Hz to 1 MHz using a Hewlett-Packard precision LCR meter (4284A). The dc conductivity was measured using two platinum electrodes as an ion-blocking electrode. For the polarization measurements, dc current of 0.1 μA was passed between the two platinum electrodes sandwiching the sample and the voltage generated was monitored as a function of time in an oxygen atmosphere (P_{O_2}: 1×10^5 Pa) and in a helium (P_{O_2}: 4 Pa) atmosphere, respectively. The oxygen pressures of 10^2 to 10^5 Pa and 10^{-12} to 10^{-15} Pa were varied by mixing air−N_2 or CO−CO_2 in the proper ratio. For the measurement in 10^5 Pa, pure O_2 gas was applied.

Electrolysis. The dc electrolysis was performed using two platinum plates as ion-blocking electrodes by applying a direct voltage of 8 V for 140 h at 800 °C in air. Since the decomposition voltage of $Sc_2(MoO_4)_3$ was identified to be ~0.5 V in a preliminary experiment, the dc electrolysis was carried out at 8 V, which is appreciably higher than the decomposition voltage. After the electrolysis, the cathodic surface of the samples was analyzed using a scanning electron microscope (SEM, S-800, Hitachi) and an electron probe microanalyzer (EPMA-1500, Shimadzu). The electrolyzed samples were mounted in an epoxy resin and then cut so that cross-sectional EPMA line analysis could be performed from the anode to cathode direction. The electrolyzed samples were then polished using a diamond paste having an average diameter of 1 μm.

Results and Discussion

From the X-ray powder diffraction analysis, all molybdates prepared were found to form $Sc_2(WO_4)_3$-type structure. In the molybdate series, the angles of the peaks shifted higher with the decrease in trivalent ion size.

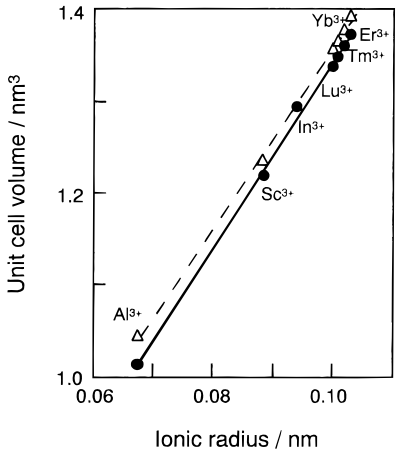

Figure 1. Trivalent ionic radius dependencies of unit cell volume for $M_2(MoO_4)_3$ (M = Al, In, Sc, Er, Tm, Yb, and Lu) (●) in addition to the data for the tungstates (△).[9]

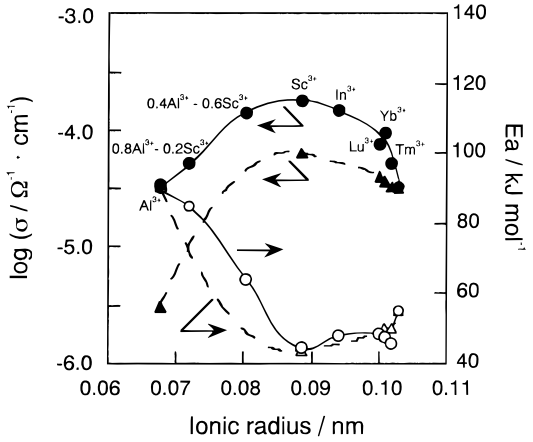

Figure 2. Trivalent ionic radius dependencies of the electrical conductivity and the activation energy (E_a) for molybdate (●, ○) and tungstate (▲, △)[9] series at 600 °C.

Figure 1 shows the trivalent ionic radius dependencies of unit cell volume for the molybdates as well as the data for the tungstate series.[9] Since the ionic radius of Mo^{6+} (0.055 nm) is smaller than that of W^{6+} (0.056 nm), the unit cell volume of the molybdate series is lower than that of the tungstate series. The slopes of the two lines in Figure 1 are almost identical due to having the same crystal structure (orthorhombic, *Pbcn*).

Trivalent ionic radius dependencies of electrical conductivity and the activation energy (E_a) are presented in Figure 2. In the present study, the $Al_2(MoO_4)_3$ −$Sc_2(MoO_4)_3$ solid solutions were also prepared to clarify the optimum ionic radius for both electrical conductivity and activation energy (E_a). The data for the tungstates[9] are also shown in Figure 2 for comparison. The electrical conductivity increased by completely replacing Al^{3+} sites with Sc^{3+} in the $Al_2(MoO_4)_3$−$Sc_2(MoO_4)_3$ solid solution. The conductivities of $Al_2(MoO_4)_3$ and $Sc_2(MoO_4)_3$ are 1 order and 6.3 times higher than those of $Al_2(WO_4)_3$ and $Sc_2(WO_4)_3$, respectively, and a maximum conductivity is observed for Sc^{3+} as the trivalent ion species in the molybdate series, which is similar to the case for the tungstate series, while $Sc_2(MoO_4)_3$ and $Sc_2(WO_4)_3$ pos-

(19) Izumi, F. *The Rietveld Method*; Oxford University Press: Oxford, 1993; Chapter 13.

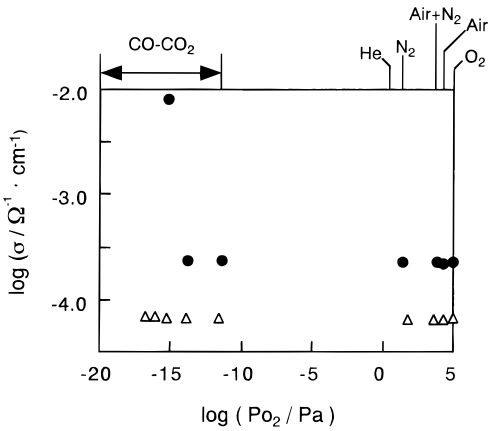

Figure 3. Oxygen pressure dependencies of the electrical conductivity of $Sc_2(MoO_4)_3$ (●) and the previously reported data[9] for the $Sc_2(WO_4)_3$ tungstates (△) at 700 °C.

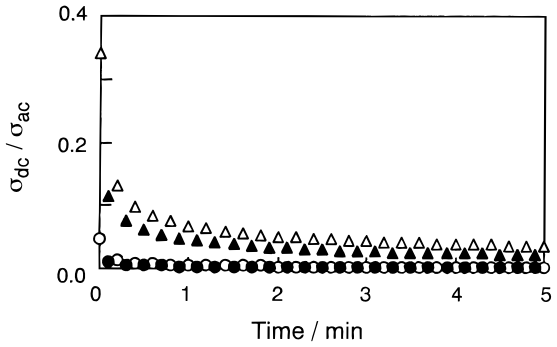

Figure 4. Time dependencies of the ratio of the electrical conductivity obtained by the dc method to that obtained by the ac method for $Sc_2(MoO_4)_3$ (○, ●) and $Sc_2(WO_4)_3$ (△, ▲) in an oxygen (open) or a helium (closed) atmosphere at 700 °C.

sess similar relative densities of 98.6% and 98.1%, respectively.

For the purpose of ensuring an electron or a hole conduction in the molybdate series, scandium molybdate, which shows the highest conductivity, was selected as the representative of the series and the oxygen pressure dependencies of the electrical conductivity were studied (Figure 3). At oxygen pressures below 10^{-13} Pa, the conductivity increased abruptly, indicating the appearance of an n-type electronic conduction. Since Mo^{6+} ions are easier to reduce in comparison to W^{6+}, the reduction of Mo^{6+} causes electronic conduction. However, over such a wide pressure region, from 10^{-13} to 10^5 Pa, the conductivity was constant. This result clearly indicates that $Sc_2(MoO_4)_3$ is stable over such a wide pressure range, including the oxygen pressure in nitrogen (Po_2: 10^2 Pa) and helium (Po_2: 4 Pa), and that no electron or hole conduction appears.

Figure 4 shows the time dependencies of the ratio of the electrical conductivity obtained by the dc method to that by the ac method (σ_{dc}/σ_{ac}) in an oxygen or a helium atmosphere. The ratio greatly decreased in both atmospheres and reached a stable state after 5 min. These high polarizing behaviors indicate that the oxide ions are excluded as the migrating species in scandium molybdate, as demonstrated in our previous paper.[9] The figure includes the data obtained for the tungstate series.[9] By comparing the data obtained for $Sc_2(MoO_4)_3$ and that obtained for $Sc_2(WO_4)_3$, a larger polarization is observed in the case of the molybdate. Since the conductivity in the molybdate, which is predominantly attributed to the trivalent ion conduction as described below, is higher than that in the tungstate, a steeper polarization was observed for $Sc_2(MoO_4)_3$. From the polarization behavior of $Sc_2(MoO_4)_3$ depicted in Figure 4, the ion transference number (t_i) for $Sc_2(MoO_4)_3$ is estimated to be higher than 0.999, showing a higher predominance of trivalent ion conducting characteristics than the case for $Sc_2(WO_4)_3$ (t_i: 0.99).[9]

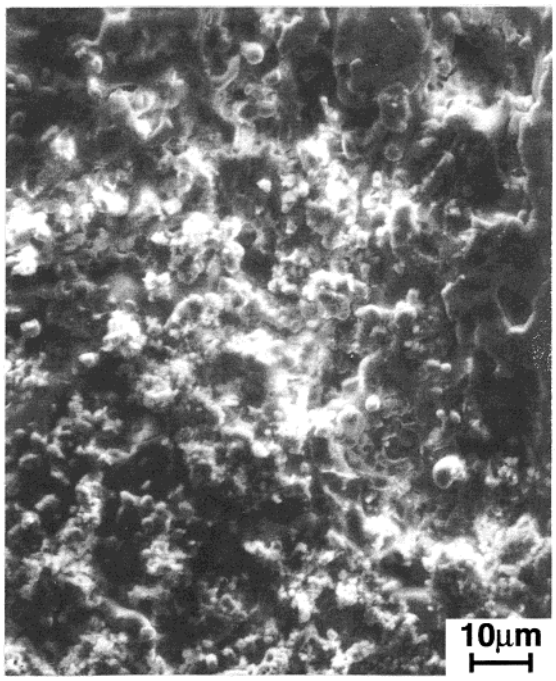

Figure 5. SEM photograph of the cathodic surface of $Sc_2(MoO_4)_3$ after electrolysis.

Table 1. Molar Ratio of Cation Species on Cathodic and Anodic Surfaces of $Sc_2(MoO_4)_3$ after Electrolysis (the data for $Sc_2(MoO_4)_3$ without electrolysis are also tabulated)

	Sc/mol %	Mo/mol %
cathode	94.2	5.8
anode	35.9	64.1
$Sc_2(MoO_4)_3$ without electrolysis	48.2	51.8

Figure 5 presents an SEM photograph of the deposits that appeared on the cathodic surface after the dc electrolysis (8 V, 800 °C, 140 h). The molar percentage of cation species on cathodic and anodic surfaces after the electrolysis is obtained by EPMA spot analysis and is presented in Table 1 together with the data for $Sc_2(MoO_4)_3$ without any electrolysis treatment. From Table 1, the predominant ion species in the deposits is clearly elemental Sc. A relatively higher Mo ratio was also observed for the anodic surface, suggesting Sc^{3+} ion migration during the electrolysis. X-ray powder diffraction analysis on the cathodic surface revealed the deposits to be Sc_2O_3.

To clarify the macroscopic Sc^{3+} ion migration and the Sc segregation near the cathodic surface area of the molybdate electrolyte, the line analysis of the $Sc_2(MoO_4)_3$ pellet was also carried out after the electrolysis and the result is presented in Figure 6. A clear Sc segregation was observed near the cathodic surface, whereas the decrease in the amount of Mo near the

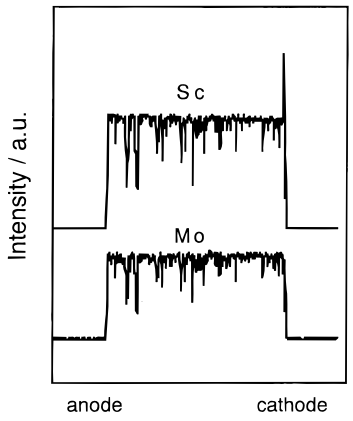

Figure 6. Cross-sectional EPMA line analysis of elemental scandium and molybdenum for the $Sc_2(MoO_4)_3$ pellet after electrolysis.

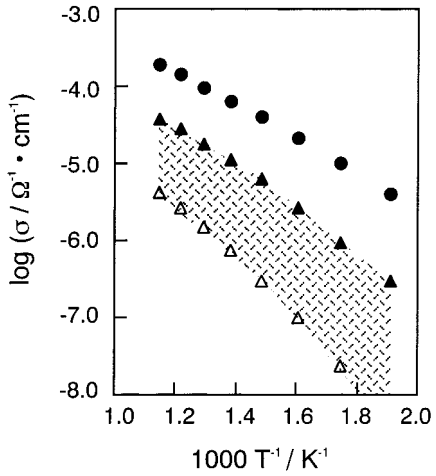

Figure 7. Temperature dependencies of the trivalent Sc^{3+} ion conductivity of scandium molybdate (●). The data for $Al_2(WO_4)_3$ (△) and $Sc_2(WO_4)_3$ (▲) that show the lowest and the highest trivalent ion conductivities in the tungstate series are also plotted for comparison.[9]

cathodic area was recognized because of the Sc segregation.

The above results clearly demonstrate the macroscopic migration of the mobile trivalent Sc^{3+} ion from the anode to cathode and the precipitation of Sc metal on the surface of the cathode. Since the electrolysis was carried out in air, the Sc metal immediately oxidized and deposited as Sc_2O_3. In contrast, on the anodic surface, no deposition was observed. By the electrolysis, Sc^{3+} ion migrated toward the cathode direction and oxygen gas was released into the ambient atmosphere, leaving molybdenum trioxide (MoO_3) on the anodic surface, because the electrolysis was performed at a higher voltage than the decomposition voltage of $Sc_2(MoO_4)_3$. Since the electrolysis was carried out at 800 °C, most of the MoO_3 that appeared on the surface vaporized into the ambient atmosphere. The above-mentioned phenomenon also refutes the hypothesis that the Sc_2O_3 that appears on the cathodic surface is formed by thermal decomposition of the $Sc_2(MoO_4)_3$ electrolyte, because if this were actually to occur, Sc_2O_3 would also be observed on the anodic surface.

Figure 7 presents the trivalent ion conductivity results for scandium molybdate, which shows the highest trivalent ion conductivity in the molybdate series, and $Al_2(WO_4)_3$ and $Sc_2(WO_4)_3$, which exhibit the lowest and the highest trivalent ion conductivity, respectively, in the tungstate series. Despite the unit cell volume shrinkage, the conductivity of $Sc_2(MoO_4)_3$ increased appreciably in comparison with that of $Sc_2(WO_4)_3$, indicating the contribution of the stronger Mo−O bonding to the enhancement of the trivalent ion conducting characteristics. Among the $Sc_2(WO_4)_3$-type structure of the molybdate and tungstate series, the relationship between the mobile ion size and the lattice volume of the $Sc_2(WO_4)_3$-type structure was clearly demonstrated.

Conclusions

Molybdates having $Sc_2(WO_4)_3$-type structure are trivalent ion conducting solid electrolytes and show a higher conductivity in comparison to the tungstate $Sc_2(WO_4)_3$-type series. The replacement of the W^{6+} site in the $Sc_2(WO_4)_3$ structure for Mo^{6+}, results in stronger bonding between the hexavalent Mo^{6+} ion and the surrounding oxide anions that form a tetrahedron and develops conditions under which trivalent ion migrates more smoothly. Among the molybdate series, $Sc_2(MoO_4)_3$ was found to have an optimum ratio of migrating trivalent ion size to molybdate crystal lattice volume of the $Sc_2(WO_4)_3$-type structure and shows the highest trivalent ion conductivity and a Sc^{3+} ion transference number of unity.

Acknowledgment. The present study was supported in part by a Grant-in-Aid for Scientific Research no. 09215223 in Priority Areas (no. 260), nos. 06241106, 06241107, and 093065 from the Ministry of Education, Science, Sports and Culture. This study was also supported by the "Research for the Future, Preparation and Application of Newly Designed Solid Electrolytes (JSPS-RFTF96P00102)" Program of the Japan Society for the Promotion of Science.

CM990591W